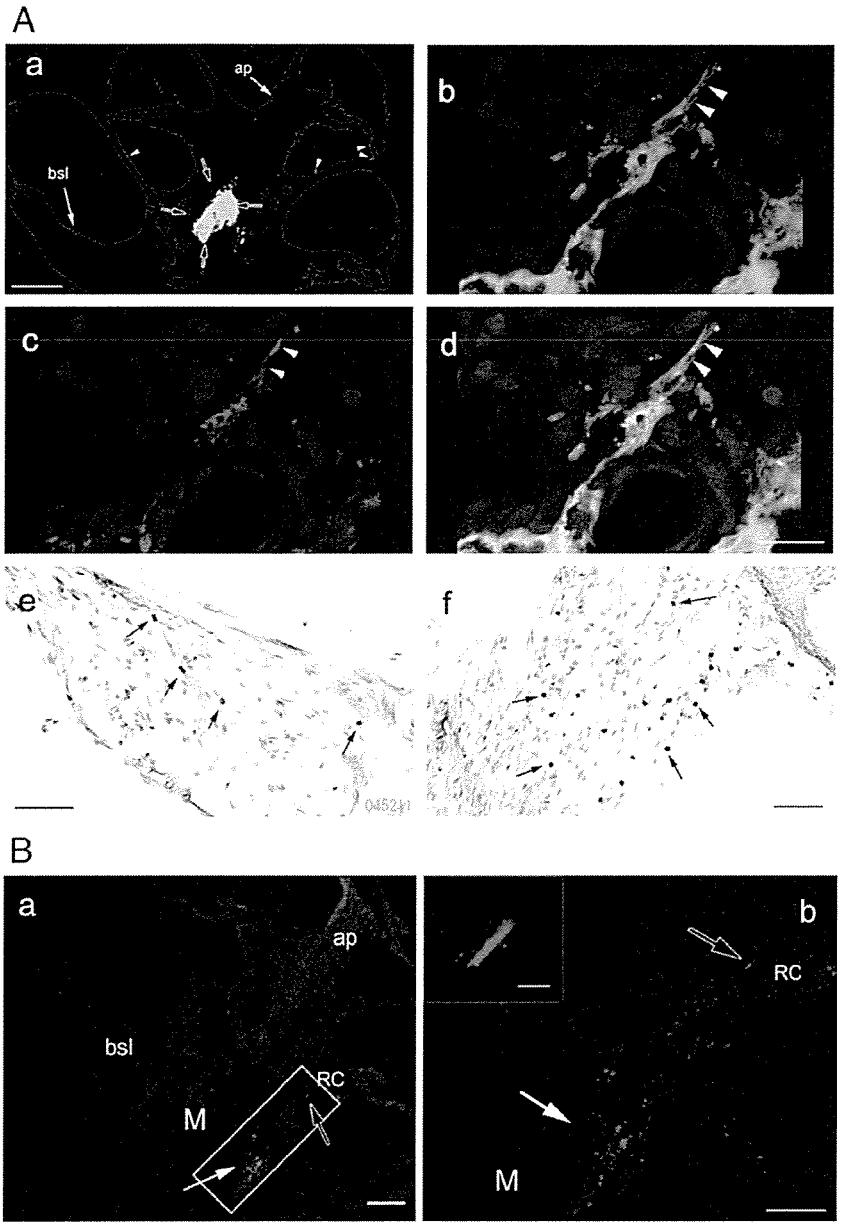


Fig. 6. ES-SDIA cells transplanted into atrophic auditory nerve trunk. (A) Histological appearance of the auditory nerve and cochlea showing transplanted ES-SDIA cells in a rat of group 2 (32 days following transplantation). (a) A relatively large cell mass was found in auditory nerve trunk (arrows). Arrow heads indicate the transplanted cells found in the scala tympani. bsl and ap, basal and apical cochlear turns, respectively. Confocal microscopy revealed an EGFP and βIII-tubulin-positive neurite process (arrow heads) among Schwann cells in b and c, respectively. These images are merged in (d) (arrow heads). The nuclei of the host tissue were stained with TOTO3. The arrows in e and f indicate DAB-positive transplanted cells in the basal and apical turns of the cochlea, respectively. Scale bars, 200, 20, 20, 20, 50, and 50 μm in a, b, c, d, e, and f, respectively. (B) Histological appearance of the auditory nerve and cochlea showing transplanted ES-SDIA cells in a rat of group 2 (35 days after transplantation). (a) A group of transplanted cells (red) was seen in the modiolus (M) (white arrow), and a neuritic process was seen in Rosenthal's canal (RC) (black arrow). Host tissue was stained blue with DAPI. bsl, basal turn; ap, apical turn. The rectangular area is enlarged in b. M, modiolus. (b) Transplanted cells (red) were found within the modiolus (M) (white arrow). A neuritic process that emerged from the bony canal (tractus spiralis foraminosus) and extended into Rosenthal's canal appeared in tangential section (black arrow). Inset: Higher magnification view of neuritic processes indicated by black arrow in b. Compare with the inset in Fig. 7B. Scale bars, 200 and 100 (20) μm in a and b, respectively.

was the remarkable ability of ES-SDIA cells to extend neuritic processes along the auditory nerve (Figs. 4B-c, 6A-b, c, d, 6B and 7). Some transplanted cells with cell bodies in the modiolus had neuritic process extending to RC (Fig. 6B-b), and cells that had migrated to the Schwann–glial junctional zone had neuritic process extending to the peripheral myelin region (Fig. 4B-c). A study that investigated regeneration of axons in the rat optic nerve revealed that axons failed to regenerate in the astrocytic environment (central myelin portion) but readily re-grew in the presence of Schwann cells (peripheral myelin portion), even across the Schwann–glial junctional zone, indicating that resident Schwann cells may exert trophic effects (Berry et al., 1992). This possibility was supported by the findings in the study we report here.

The survival rates of various cells transplanted into the inner ear spaces have been reported to be quite low and no more than

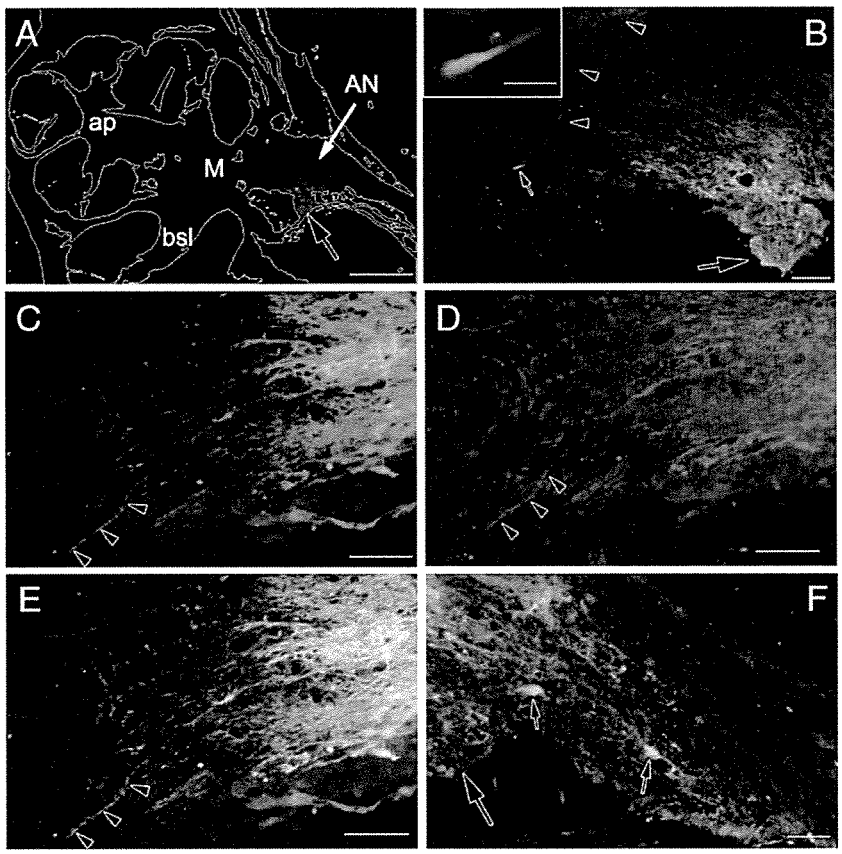


Fig. 7. Histological appearance of the auditory nerve and cochlea showing ES-SDIA cells that had been transplanted to an intact auditory nerve (AN). (A) An EGFP-positive cell mass (black arrow) was seen at the transplantation site in the auditory nerve. bsl, basal turn; ap, apical turn; M, modiolus. (B) Transplanted cell mass (larger arrow) extended neurites distally, and one neurite was found to have extended into the peripheral myelin portion of the auditory nerve trunk (smaller arrow, shown enlarged in the inset). The tip of the neurite had the shape of a growth cone (inset; compare with Fig. 6B-b). Arrow heads indicate the dome-shaped Schwann–glial junctional zone. (C, D) Neurite extensions stained with anti-EGFP (C) and βIII-tubulin (D) staining. One neurite extended into quite a distance into the peripheral myelin portion (arrow heads). (E) Merged view. (F) Neurite extensions and a few cell bodies were also found proximal to the cell transplantation site (smaller black arrows), and a cell mass (larger arrow) was seen attached to the auditory nerve. Host cells stained blue with DAPI in B, C, D, E and F. Scale bars, 500, 50 (20), 100, 100, 100, and 50 μm in A, B (inset), C, D, E, and F, respectively.

2.0% (Hu et al., 2004a,b). It is difficult to make an accurate estimate of survival of transplanted cells. However, the survival rate seems to vary according to the method; intra-neurally transplanted cells (Fig. 6A) seemed to survive more than peri-neurally transplanted cells (Figs. 4, 5). In future studies, we should select appropriate cells with or without some adjunct therapies such as pre-conditioning with neurotrophic factors. It might be beneficial to add some neurotrophic factors such as NGF to foster neurite outgrowth from the cells transplanted to the injured auditory nerve (Hu et al., 2005).

In xenograft transplantation, some immunosuppressant may be beneficial to secure the transplanted cells at the host, although, in the present study, we did not apply this strategy. Refinement of the delivery technique to maximize the survival of transplanted cells and to enhance neuronal differentiation will be investigated in our future studies.

*Selective ablation of the auditory neurons with hair cells spared*

We found that the hair cells did not degenerate within 4 weeks of damage to the auditory neurons (Figs. 2B, C). Our previous study indicated that the auditory neurons from the apical cochlear turn were injured more than those from more basal cochlear turns in our experimental model (Sekiya et al., 2000). This might have been one of the reasons why some limited signs of hair cell loss were observed in the apical region. In future studies, we could selectively ablate groups of auditory neurons by applying a weaker compression force than used in the present study. Compression injury is precise and does not involve the more widespread and non-specific effects that may occur with pharmacologic methods (Lang et al., 2005; Schmiedt et al., 2002). Taken together, this model may provide unique opportunities to investigate the regeneration of spiral ganglion neurons without being confounded by the changes occurred in the hair cell region.

*Candidate materials for cell transplantation therapy to rebuild lost hearing*

One reason why we used ES-SDIA cells in this particular study was that they had been induced in advance to differentiate into neural cells versus endo- or mesodermal cells. Other cells, however, could be candidates for transplantation to rebuild lost hearing (Fuchs and Segre, 2000; Morest and Cotanche, 2004).

For example, tissue-specific stem cells derived from inner ear tissue (Bermingham-McDonogh and Rubel, 2003; Germiller et al., 2004; Kalinec et al., 1999; Kojima et al., 2004; Lawoko-Kerali et al., 2004; Li et al., 2003; Nicholl et al., 2005; Rask-Andersen et al., 2005; Rivolta and Holley, 2002) would be expected to have a high possibility of being morphologically and functionally integrated into a host's inner ear.

To avoid problems with tissue rejection, autologous cells such as bone marrow stromal cells could be useful (Munoz-Elias et al., 2004; Ohta et al., 2004). A second possibility is to transplant cells, such as those carrying potentially beneficial genes (such as genes promoting hair cell regeneration or secreting neurotrophins that would enhance the function of existing cells). It would not be necessary for such transplanted cells to be morphologically integrated into the host tissue. Rather, it might be sufficient for them to "float" in the target area such as the endolymphatic space. A third possibility is to deliver neurotrophins, growth factors, or pharmacological agents by placing these materials at the IAM portion of the auditory nerve using drug delivery systems.

*Our technique is clinically feasible*

Clinically, we can enter into the CP angle using retromastoid craniectomy through an incision behind the ear and place various materials at the IAM portion of the auditory nerve in human. This approach is currently used clinically in a variety of procedures, such as microvascular decompression to treat hemifacial spasm, trigeminal neuralgia, and resection of tumors in the CP angle, including vestibular schwannomas (McLaughlin et al., 1999; Ojemann, 2001; Samii and Matthies, 1997; Sanna et al., 2004). In contrast to the cochlea in small experimental animals such as rat, mouse, and guinea pig, where the cochlear wall is directly sighted in the tympanic bulla, the human cochlea is embedded deep in the temporal bone. Therefore, in order to reach the cochlea wall in humans, the thick bone around the cochlea should be removed without damaging intracochlear structures. This seemed to be quite a difficult task to be performed in comparison with the technique through the CP angle in our technique. Other advantages of our technique include its versatility. For example, when transplantation of cells into the cochlear nucleus region is planned (Hu et al., 2004a), cells can be placed in this region under direct visual control. In contrast to an extensive migration of the transplanted cells towards the regions distal to the transplanted site in this study, we found a very few cells centrally. It is not clear why relatively few cells migrated into the brainstem regions.

We believe that through collaboration and use of techniques such as those reported here, experts in molecular cell engineering, neuro-otology, and neurosurgery will be able to offer hope to many patients with profound hearing disturbances.

## Acknowledgments

This work was supported by the Japanese Ministry of Education, Culture, Sports, Science, and Technology. We appreciate Dr. Hiroshi Niwa, Riken Center for Developmental Biology, Kobe, for his generous gift of ES cells used in this study. Anti-myosin VIIa antibody was kindly provided by Dr. Tama Hasson, University of California at San Diego, CA, USA. Professor Matthew C. Holley, Department of Biomedical Sciences, the University of Sheffield, critically reviewed the manuscript. We are grateful to Drs. Tatsunori Sakamoto, Harukazu Hiraumi, Shinichiro Kitajiri, and Anthony FW Foong for their valuable discussion and Drs. Takayuki Nakagawa, Tomoko Kita, and Tsuyoshi Endo for their help with preparation of experimental equipment. Thanks are due to Ms. Yoko Nishiyama, Rika Sadato, and Mami Kubota for their technical expertise. Diana B. Mathis, BSN, ELS, edited the manuscript. The authors declare that they have no competing financial interests.

## References

Bermingham-McDonogh, O., Rubel, E.W., 2003. Hair cell regeneration: winging our way towards a sound future. Curr. Opin. Neurobiol. 13, 119–126.

Berry, M., Hall, S., Rees, L., Carlile, J., Wyse, J.P., 1992. Regeneration of axons in the optic nerve of the adult Browman–Wyse (BW) mutant rat. J. Neurocytol. 21, 426–448.

Bianchi, L.M., Raz, Y., 2004. Methods for providing therapeutic agents to treat damaged spiral ganglion neurons. Curr. Drug Targets. CNS Neurol. Disord. 3, 195–199.

Brown, J.N., Miller, J.M., Altschuler, R.A., Nuttall, A.L., 1993. Osmotic pump implant for chronic infusion of drugs into the inner ear. Hear. Res. 70, 167–172.

Fricker, R.A., Carpenter, M.K., Winkler, C., Greco, C., Gates, M.A., Bjorklund, A., 1999. Site-specific migration and neuronal differentiation of human neural progenitor cells after transplantation in the adult rat brain. J. Neurosci. 19, 5990–6005.

Fuchs, E., Segre, J.A., 2000. Stem cells: a new lease on life. Cell 100, 143–155.

Germiller, J.A., Smiley, E.C., Ellis, A.D., Hoff, J.S., Deshmukh, I., Allen, S.J., Barald, K.F., 2004. Molecular characterization of conditionally immortalized cell lines derived from mouse early embryonic inner ear. Dev. Dyn. 231, 815–827.

Holley, M.C., 2002. Application of new biological approaches to stimulate sensory repair and protection. Br. Med. Bull. 63, 157–169.

Hoshino, T., Hiraide, F., Nomura, Y., 1972. Metastatic tumour of the inner ear: a histopathological report. J. Laryngol. Otol. 86, 697–707.

Hu, Z., Ulfendahl, M., Olivius, N.P., 2004a. Central migration of neuronal tissue and embryonic stem cells following transplantation along the adult auditory nerve. Brain Res. 1026, 68–73.

Hu, Z., Ulfendahl, M., Olivius, N.P., 2004b. Survival of neuronal tissue following xenograft implantation into the adult rat inner ear. Exp. Neurol. 185, 7–14.

Hu, Z., Ulfendahl, M., Olivius, N.P., 2005. NGF stimulates extensive neurite outgrowth from implanted dorsal root ganglion neurons following transplantation into the adult rat inner ear. Neurobiol. Dis. 18, 184–192.

Ito, J., Kojima, K., Kawaguchi, S., 2001. Survival of neural stem cells in the cochlea. Acta Oto-Laryngol. 121, 140–142.

Izumikawa, M., Minoda, R., Kawamoto, K., Abrashkin, K.A., Swiderski, D.L., Dolan, D.F., Brough, D.E., Raphael, Y., 2005. Auditory hair cell replacement and hearing improvement by Atoh1 gene therapy in deaf mammals. Nat. Med. 11, 271–276.

Kalinec, F., Kalinec, G., Boukhvalova, M., Kachar, B., 1999. Establishment and characterization of conditionally immortalized organ of corti cell lines. Cell Biol. Int. 23, 175–184.

Kawasaki, H., Mizuseki, K., Nishikawa, S., Kaneko, S., Kuwana, Y., Nakanishi, S., Nishikawa, S.I., Sasai, Y., 2000. Induction of midbrain dopaminergic neurons from ES cells by stromal cell-derived inducing activity. Neuron 28, 31–40.

Kojima, K., Tamura, S., Nishida, A.T., Ito, J., 2004. Generation of inner ear hair cell immunophenotypes from neurospheres obtained from fetal rat central nervous system in vitro. Acta Oto-Laryngol. 26–30.

LaBarge, M.A., Blau, H.M., 2002. Biological progression from adult bone marrow to mononucleate muscle stem cell to multinucleate muscle fiber in response to injury. Cell 111, 589–601.

Lang, H., Schulte, B.A., Schmiedt, R.A., 2005. Ouabain induces apoptotic cell death in Type I spiral ganglion neurons, but not type II neurons. J. Assoc. Res. Otolaryngol. 6, 63–74.

Lawoko-Kerali, G., Milo, M., Davies, D., Halsall, A., Helyer, R., Johnson, C. M., Rivolta, M.N., Tones, M.A., Holley, M.C., 2004. Ventral otic cell lines as developmental models of auditory epithelial and neural precursors. Dev. Dyn. 231, 801–814.

Li, H., Liu, H., Heller, S., 2003. Pluripotent stem cells from the adult mouse inner ear. Nat. Med. 9, 1293–1299.

McLaughlin, M.R., Jannetta, P.J., Clyde, B.L., Subach, B.R., Comey, C.H., Resnick, D.K., 1999. Microvascular decompression of cranial nerves: lessons learned after 4400 operations. J. Neurosurg. 90, 1–8.

Minor, L.B., 2003. Labyrinthine fistulae: pathobiology and management. Curr. Opin. Otolaryngol. Head Neck Surg. 11, 340–346.

Morest, D.K., Cotanche, D.A., 2004. Regeneration of the inner ear as a model of neural plasticity. J. Neurosci. Res. 78, 455–460.

Morest, D.K., Kim, J., Bohne, B.A., 1997. Neuronal and transneuronal degeneration of auditory axons in the brainstem after cochlear lesions in the chinchilla: cochleotopic and non-cochleotopic patterns. Hear. Res. 103, 151–168.

Munoz-Elias, G., Marcus, A.J., Coyne, T.M., Woodbury, D., Black, I.B., 2004. Adult bone marrow stromal cells in the embryonic brain: engraftment, migration, differentiation, and long-term survival. J. Neurosci. 24, 4585–4595.

Nicholl, A.J., Kneebone, A., Davies, D., Cacciabue-Rivolta, D.I., Rivolta, M. N., Coffey, P., Holley, M.C., 2005. Differentiation of an auditory neuronal cell line suitable for cell transplantation. Eur. J. Neurosci. 22, 343–353.

Ohta, M., Suzuki, Y., Noda, T., Ejiri, Y., Dezawa, M., Kataoka, K., Chou, H., Ishikawa, N., Matsumoto, N., Iwashita, Y., Mizuta, E., Kuno, S., Ide, C., 2004. Bone marrow stromal cells infused into the cerebrospinal fluid promote functional recovery of the injured rat spinal cord with reduced cavity formation. Exp. Neurol. 187, 266–278.

Ojemann, R.G., 2001. Retrosigmoid approach to acoustic neuroma (vestibular schwannoma). Neurosurgery 48, 553–558.

Pujol, R., Puel, J.L., Gervais d'Aldin, C., Eybalin, M., 1993. Pathophysiology of the glutamatergic synapses in the cochlea. Acta Oto-Laryngol. 113, 330–334.

Rask-Andersen, H., Bostrom, M., Gerdin, B., Kinnefors, A., Nyberg, G., Engstrand, T., Miller, J.M., Lindholm, D., 2005. Regeneration of human auditory nerve. In vitro/in video demonstration of neural progenitor cells in adult human and guinea pig spiral ganglion. Hear. Res. 203, 180–191.

Regala, C., Duan, M., Zou, J., Salminen, M., Olivius, P., 2005. Xenografted fetal dorsal root ganglion, embryonic stem cell and adult neural stem cell survival following implantation into the adult vestibulocochlear nerve. Exp. Neurol. 193, 326–333.

Rivolta, M.N., Holley, M.C., 2002. Cell lines in inner ear research. J. Neurobiol. 53, 306–318.

Sakamoto, T., Nakagawa, T., Endo, T., Kim, T.S., Iguchi, F., Naito, Y., Sasai, Y., Ito, J., 2004. Fates of mouse embryonic stem cells transplanted into the inner ears of adult mice and embryonic chickens. Acta Oto-Laryngol. 48–52 (Suppl.).

Samii, M., Matthies, C., 1997. Management of 1000 vestibular schwannomas (acoustic neuromas): hearing function in 1000 tumor resections. Neurosurgery 40, 248–260 (discussion 260–242).

Sanna, M., Taibah, A., Russo, A., Falcioni, M., Agarwal, M., 2004. Perioperative complications in acoustic neuroma (vestibular schwannoma) surgery. Otol. Neurotol. 25, 379–386.

Schmiedt, R.A., Okamura, H.O., Lang, H., Schulte, B.A., 2002. Ouabain application to the round window of the gerbil cochlea: a model of auditory neuropathy and apoptosis. J. Assoc. Res. Otolaryngol. 3, 223–233.

Sekiya, T., Hatayama, T., Shimamura, N., Suzuki, S., 2000. An in vivo quantifiable model of cochlear neuronal degeneration induced by central process injury. Exp. Neurol. 161, 490–502.

Sekiya, T., Yagihashi, A., Shimamura, N., Asano, K., Suzuki, S., Matsubara, A., Namba, A., Shinkawa, H., 2003. Apoptosis of auditory neurons following central process injury. Exp. Neurol. 184, 648–658.

Spoendlin, H., 1987. The afferent innervation of the cochlea. In: Naunton, F.R., C (Eds.), Evoked Electrical Activity in the Auditory Nervous System. Academic Press, New York, pp. 21–41.

Staecker, H., Li, D., O'Malley Jr., B.W., Van De Water, T.R., 2001. Gene expression in the mammalian cochlea: a study of multiple vector systems. Acta Otolaryngol. 121, 157–163.

Starr, A., Picton, T.W., Sininger, Y., Hood, L.J., Berlin, C.I., 1996. Auditory neuropathy. Brain 119 (Pt. 3), 741–753.

Yagihashi, A., Sekiya, T., Suzuki, S., 2005. Macrophage colony stimulating factor (M-CSF) protects spiral ganglion neurons following auditory nerve injury: morphological and functional evidence. Exp. Neurol. 192, 167–177.

STEM CELLS AND DEVELOPMENT 15:566–574 (2006)
© Mary Ann Liebert, Inc.

# Original Research Report

# Molecular Cloning and Function of Oct-3 Isoforms in Cynomolgus Monkey Embryonic Stem Cells

YASUKO FUJIMOTO,[1–3] KOUICHI HASEGAWA,[1,2] HIROFUMI SUEMORI,[1] JUICHI ITO,[3] and NORIO NAKATSUJI[2]

## ABSTRACT

**Oct-3 is a key molecule for maintaining self-renewal in mouse embryonic stem (ES) cells. The function of Oct-3 in ES cells of other species, however, especially primate ES cells, is not clear. In the present study, we cloned two splicing isoforms of Oct-3, Oct-3A and Oct-3B, from cynomolgus monkey ES cells, and found that they have high homology to human Oct-3A and Oct-3B. To examine their function, Oct-3A and Oct-3B were overexpressed in cynomolgus monkey ES cells. Transient Oct-3A overexpression induced ES cell differentiation into endodermal and mesodermal lineages and disrupted proliferation of undifferentiated monkey ES cells. In contrast, Oct-3B overexpression did not induce differentiation of monkey ES cells. These findings indicate that a certain Oct-3A expression level has an important role in sustaining self-renewal in non-human primate ES cells.**

## INTRODUCTION

EMBRYONIC STEM (ES) CELLS are derived from the inner cell mass (ICM) of preimplantation embryos (1). Mouse ES cell lines, which were first established in 1981 by Evans and Kaufman (1), have the capacity to differentiate into all cell types derived from the three primary germ layers, and are capable of long-term renewal in vitro (2). Non-human primate ES cell lines were established from rhesus monkey in 1995 (3), common marmoset in 1996 (4), and cynomolgus monkey in 2001 (5). Human ES cell lines were established in 1998 (6). Human ES cells are expected to be powerful and promising tools for regenerative medicine, and non-human primate ES cells, which are more closely related to human ES cells than rodent ES cells, are expected to be valuable preclinical models. Most research, however, has been limited to application in rodent models. Studies in which primate ES cells have been applied to primate disease models are limited (7). Verifying the effects and safety of new methods in non-human primates is an indispensable intermediary step for regenerative medicine before applying new therapeutic strategies to humans.

Although previous research indicates that primate ES cells have a differentiation potency similar to that of mouse ES cells, there are several differences between primate and mouse ES cells. For example, the role of the signaling pathways in ES cell self-renewal, such as the LIF/JAK/Stat3 pathway (8–11) and the BMP/ Id pathway, differs between mouse and primate ES cells (12–14). It is, therefore, important to clarify the mechanisms through which self-renewal of primate ES cells is stably maintained to apply it to large-scale preclinical research.

[1]Laboratory of Embryonic Stem Cell Research, Stem Cell Research Center, [2]Department of Development and Differentiation, Institute for Frontier Medical Sciences, Kyoto University, 606-8507, Japan.

[3]Department of Otolaryngology, Head and Neck Surgery, Graduate School of Medicine, Kyoto University, Kyoto, 606-8507, Japan.

The POU transcription factor Oct-3 (also known as Oct-4, Oct-3/4, encoded by *POU5F1*) (15–17) functions as a key molecule in maintaining pluripotency and germline development in mammals (18,19). Oct-3 is expressed in totipotent and pluripotent cells in oocytes and pregastrulation embryos, and it is also highly expressed in ES, embryonic carcinoma, and embryonic germ cell lines (20–24). In mouse ES cells, a certain amount of Oct-3 is critical for maintaining ES cell self-renewal, and any up- or down-regulation induces various cell fates. Using a tetracycline-regulated Oct-3 expression system, Niwa and colleagues showed that decreasing Oct-3 expression to less than half in mouse ES cells drives formation of trophectoderm lineage cells, and increasing Oct-3 expression by more than half increases differentiation into primitive endoderm and mesoderm lineage cells (19).

In humans, there are two splicing isoforms of Oct-3 mRNA, Oct-3A and Oct-3B (25), that have not been reported in mouse. Oct-3A is considered to be the human ortholog of mouse Oct-3, and shares 87% amino acid identity with mouse Oct-3 (25). Oct-3B is a minor splicing variant form of Oct-3A mRNA. Oct-3A and Oct-3B comprise 360 and 265 amino acids, respectively, and share a 225-amino-acid sequence at their carboxy-terminal region, including the POU-specific and POU homeodomains. Oct-3B lacks the proline-rich region of Oct-3A at its amino-terminal region, which is reported to have transcriptional activity in mouse ES cells (26,27).

There have only been a few studies of Oct-3B. Takeda et al. first reported that Oct-3B mRNA was expressed in adult human tissues at low levels, but some of the population would be assumed to have no Oct-3B expression because of polymorphisms in the *POU5F1* codon (25). Caufmann et al. reported that Oct-3B in human blastocysts is localized in the cytoplasm rather than in the nucleus, whereas Oct-3A is highly concentrated in the nucleus (28). Both authors presumed a functional difference between the Oct-3 isoforms in humans, but there have been no reports on the expression of the Oct-3 isoform or the functional difference between Oct-3A and Oct-3B in primate ES cells, including human ES cells.

The function of Oct-3 in primate ES cells is far from fully understood compared with that in mouse ES cells. There have been two reported Oct-3 knockdown experiments in human ES cells, both of which resulted in cell differentiation into the endoderm lineage (29,30). One of these studies reported cell differentiation into the trophectoderm lineage (30), whereas the other did not (29). These studies were performed using small interference (si) RNA that worked on both Oct-3A and Oct-3B, and thus were not capable of distinguishing between the functions of the isoforms. Furthermore, overexpression experiments of each isoform have not been performed, although they are indispensable for fully understanding Oct-3 function in the self renewal of primate ES cells.

In this report, we cloned Oct-3 isoforms in cynomolgus monkey ES cells and quantified the expression of each protein by western blotting. In monkey, as in humans, there are two Oct-3 isoforms; thus, monkey ES cells are a good model of human ES cells. We demonstrated that Oct-3A overexpression in cynomolgus ES cells induced differentiation toward endodermal and mesodermal lineages, whereas that of Oct-3B did not.

## MATERIALS AND METHODS

### *Cell culture*

A cynomolgus monkey ES cell line, CMK6, was cultured as previously described (5). Briefly, the cells were maintained on a feeder layer of mouse embryonic fibroblasts (MEFs) treated with mitomycin C in Dulbecco's modified Eagle's medium/Nutrient Mixture F12 Ham (DMEM/F12) (Sigma Aldrich, St. Louis, MO) supplemented with 20% knockout serum replacement (KSR) (Invitrogen, Carlsbad, CA), 0.1 mM 2-mercaptoethanol, 1 mM minimal essential medium (MEM) nonessential amino acids, 2 mM L-glutamine, and 1 mM sodium pyruvate.

Mouse R1 ES cells (31) were cultured on MEFs in DMEM/F12 supplemented with 15% fetal bovine serum (FBS; HyClone, Boston, MA), 0.1 mM 2-mercaptoethanol, 2 mM L-glutamine, 1 mM sodium pyruvate, 1 mM MEM nonessential amino acids, and 1,000 U/ml recombinant mouse leukemia inhibitory factor (LIF) (Chemicon International, Temecula, CA).

### *Cloning of monkey Oct-3 cDNA*

The specific primers for the open reading frames (ORFs) of human Oct-3A and Oct-3B had the following sequences. Oct-3A-specific forward primer, 5′-ATGGCGGGACACCTGGCTTC -3′; Oct-3B-specific forward primer, 5′-AGGCAGATGCACTTCTACAGAC-3′; common reverse primer for the Oct-3 isoforms, 5′-AGGCAGGCACCTCAGTTTGAATG-3′.

Using these primers, the ORFs of monkey Oct-3 were amplified by reverse transcription (RT) PCR with mRNA from CMK6 ES cells. The PCR products were ligated into a pGEM-T easy vector (Promega, Madison, WI), and these sequences were confirmed by nucleotide sequence analysis.

### *Plasmid construction*

Oct-3A and Oct-3B overexpression vectors, driven by a CAG promoter, which is a strong promoter in mammals (32), were created by inserting the Oct-3A and Oct-3B ORFs into pCAG/PGKneo vectors (10). pCAG/PGK-

neo vectors without an Oct-3 component were used as mock transfection vectors (Mock).

### *Introduction of expression vectors into monkey and mouse ES cells*

To establish stable transfected cynomolgus monkey ES clones, transfection to cynomolgus ES cells was performed as follows. On 60-mm feeder dishes, $2.4 \times 10^5$ CMK6 cells were plated 16 h prior to transfection and were transfected for 2 h with Opti-MEM (Invitrogen) containing linearized plasmid DNA in complex with 20 $\mu$l of Lipofectamine 2000 (Invitrogen). To ensure introduction of an equal number of vector molecules, 10 $\mu$g of Oct-3A or Oct-3B expression vectors, and 8 $\mu$g of Mock vector were used for each transfection. After selection in the presence of 100 $\mu$g/ml G418 (Sigma Aldrich) for 10 days, resistant colonies were counted or recovered and plated on new feeder layers.

The mouse R1 ES cells were trypsinized and resuspended in phosphate-buffered saline (PBS), and $1 \times 10^7$ cells were electroporated with linearized plasmid DNA at 250 V and 500 $\mu$F in a 0.4-cm cuvette using a Gene Pulser (Bio-Rad, Hercules, CA). The amounts of the plasmids were 25 $\mu$g each of Oct-3A and Oct-3B expression vectors and 20 $\mu$g of Mock vector. Cells were cultured on 100-mm gelatin-coated dishes in the presence of 200 $\mu$g/ml G418 for 7 days, and the number of colonies was counted.

### *Alkaline phosphatase staining*

ES cells were fixed with 3.7% formaldehyde in PBS for 20 min at room temperature, and alkaline phosphatase (ALP) activity was detected with Vector Red substrate (Vector Laboratories, Burlingame, CA).

### *Immunoblot analysis*

To remove feeder cells, ES cells were plated on MEF extracellular matrix (ECM)-coated dishes (10). The cells were lysed in 100 $\mu$l of lysis buffer containing 50 mM Tris-HCl, pH 7.5, 0.15 M NaCl, 25 mM $\beta$-glycerophosphate, 10 mM NaF, 1 mM $Na_3VO_4$, 1% Triton X-100, 10% glycerol, and the protease inhibitor cocktail, Complete Mini (Roche, Switzerland).

The lysate samples were separated by sodium dodecyl sulfate-polyacrylamide gel electrophoresis (SDS-PAGE), electroblotted onto an Immun-Blot PVDF Membrane (Bio-Rad), and probed with primary antibodies. After incubation with horseradish peroxidase (HRP)-conjugated secondary antibodies (Dako Cytomation, Denmark), proteins reacting with antibodies were detected using enhanced chemiluminescence reagent (Western Blotting Luminol Reagent; Santa Cruz Biotechnology, Santa Cruz, CA), and analyzed by autoradiography. Anti-Oct4 (Oct-3) polyclonal antibodies (AB-3209, Chemicon International) whose epitope is common to Oct-3A and Oct-3B were used to detect both isoforms on the same membrane with different exposure times. The standardization of the samples was performed using anti-$\beta$-actin monoclonal (AC-15) antibody (A-5441, Sigma Aldrich). Signal intensity was measured using pixel intensity analysis with Scion Image software (Scion Corporation, http://www.scioncorp.com/).

### *Formation of embryoid bodies of monkey ES cells*

Cynomolgus ES cells were treated with 0.25% trypsin supplemented with 1 mM $CaCl_2$ and 20% KSR (5) and detached from feeder cells by gentle pipetting to avoid dissociation of colonies. The cells were cultured in suspension in petri dishes and aggregated to form embryoid bodies (EBs). EBs were grown in ES medium for 10 days and collected for preparation of total RNA.

### *Transient transfection and RT-PCR analysis*

For transient transfection with the expression vectors, $1.2 \times 10^5$ cynomolgus ES cells cultured on a feeder layer in 35-mm dishes were transfected with 5 $\mu$g of either Oct-3A or Oct-3B expression plasmid, or alternatively, with 4 $\mu$g mock plasmid, in 10 $\mu$l of Lipofectamine 2000. They were cultured initially for 2 h, then, after the medium was replaced, samples were collected at 24 and 48 h.

Total RNA was extracted from ES cells or from 10-day-old wild-type EBs using Trizol (Invitrogen), according to the manufacturer's protocol. Total RNA was then treated with DNase I (Takara Biotechnology, Japan), and cDNA was synthesized from 2 $\mu$g of total RNA using an RNA PCR kit (AMV) Ver3.0 (Takara Biotechnology).

Ex Taq polymerase (Takara Biotechnology) was used for the PCR reactions, which were then optimized to allow for semiquantitative comparisons within the log phase of amplification. The gene-specific primers, listed in Table 1, were designed based on published human mRNA sequences and did not cross-react with the mouse feeder cells.

## RESULTS

### *Cloning of Oct-3A and Oct-3B from monkey ES cells*

To examine whether Oct-3 isoforms exist in monkey ES cells, we performed RT-PCR cloning using variant-specific primers designed from human Oct-3A and Oct-3B cDNA, and obtained two types of cDNA clones. The

TABLE 1. PRIMERS USED IN RT-PCR STUDIES

| *Gene* | *Primer sequence (5′ → 3′)* | *Annealing temperature (°C)* | *Cycles* | *Product size (bp)* |
|---|---|---|---|---|
| *albumin* | for-GCATCCTGATTACTCTGACATG<br>rev-CTTGGTGTAACGAACTAATTGC | 58°C | 32 | 229 |
| *AFP* | for-TCAGTGAGGACAAACTATTGGC<br>rev-CACCCTGAGCTTGACACAGA | 56°C | 25 | 262 |
| *goosecoid* | for-GCTTCTCAACCAGCTGCAC<br>rev-TGCTGATGATCTTGAGGCT | 60°C | 33 | 250 |
| *Cdx2* | for-TCACCATCCGGAGGAAAGCC<br>rev-AGAGGTGCAGCCTGCAGATC | 65°C | 32 | 670 |
| *NF68kD* | for-GGCGCGCTATGAAGAGGAG<br>rev-CTTGGCCTTGAGCAGACGA | 55°C | 33 | 422 |
| *Oct-3A* | for-ATGGCGGGACACCTGGCTTC<br>rev-AGGCAGGCACCTCAGTTTGAATG | 65°C | 25 | 1094 |
| *Oct-3B* | for-AGGCAGATGCACTTCTACAGAC<br>rev-AGGCAGGCACCTCAGTTTGAATG | 65°C | 25 | 815 |
| *GAPDH* | for-ACCAGGGCTGCTTTTAACTC<br>rev-TTGCTGATGATCTTGAGGCT | 60°C | 22 | 215 |

for- and rev- stand for forward primer and reverse primers, respectively.

cDNA amplified with human Oct-3A specific primers was 1,083 bp and the cDNA amplified with human Oct-3B specific primers was 798 bp. These cDNA clones were the same size as the reported ORFs of human Oct-3A and Oct-3B, and had highly homologous nucleic acid sequences (98.2% and 98.6%, respectively) and deduced amino acid sequences (98.6% and 98.5%, respectively) (Fig. 1A,B). These two products were, therefore, considered to be the ORFs of monkey Oct-3A and Oct-3B because they have a common structure in the last 678 bp. Thus, they were considered to be splicing variant isoforms, as reported in humans. Similar to mouse Oct-3 and human Oct-3A, monkey Oct-3A has a proline-rich domain at the amino terminal, which is a transcription activation domain in mouse ES cells (26,27). In contrast, Oct-3B lacks this domain. To confirm the expression of Oct-3A and Oct-3B proteins in monkey ES cells, we performed western blot analysis using anti-Oct-3 antibodies that recognize the carboxyl termini of human Oct-3 shared by both isoforms. Both Oct-3A and Oct-3B were detected in monkey ES cells (Fig. 1C). Protein expression of Oct-3B in monkey ES cells, however, was much lower than that of Oct-3A.

### *Establishment of stable transfectants of Oct-3A or Oct-3B overexpression vectors*

Because up-regulation of Oct-3 by 50% above the normal level promotes differentiation of mouse ES cells into primitive endodermal or mesodermal lineages (19), we constructed and transfected Oct-3A and Oct-3B overexpression vectors to examine whether a particular Oct-3 expression range is required for maintaining undifferentiated states in monkey ES cells. We first electroporated these vectors into mouse ES cells to estimate whether the vectors were functional. After 1 week of G418 selection, 75% of the surviving colonies in Oct-3A-transfected mouse ES cells were completely differentiated, whereas only 10% of colonies were completely differentiated in Mock and Oct-3B transfected cells (Fig. 2A,C). This finding suggested that Oct-3 protein produced from the vectors is functional, and that, like mouse Oct-3, overexpression of Oct-3A, but not Oct-3B, affects the self-renewal of mouse ES cells.

Next, we transfected these vectors into cynomolgus monkey ES cells. Unlike the results obtained using mouse ES cells, the ratio of undifferentiated and differentiated colonies in these transfected monkey ES cells was not significantly different among the plasmids, and most of the colonies of each of the transfected cells were undifferentiated (Fig. 2D,G). The total number of surviving colonies in Oct-3A- and Oct-3B-transfected cells, however, was smaller than that in mock-transfected cells (Fig. 2F), and this was also observed in the case of mouse ES cells (Fig. 2B). To examine whether this reduction in colony numbers resulted from differences in plasmid transfection efficiency or differences in the effects of Oct-3A and Oct-3B overexpression, we performed a transfection assay using vectors linearized at the *Xba*I site. This site is located at the junction of the promoter and either Oct-3A or Oct-3B cDNA to avoid expression of exogenous Oct-3A or Oct-3B from the vectors. There

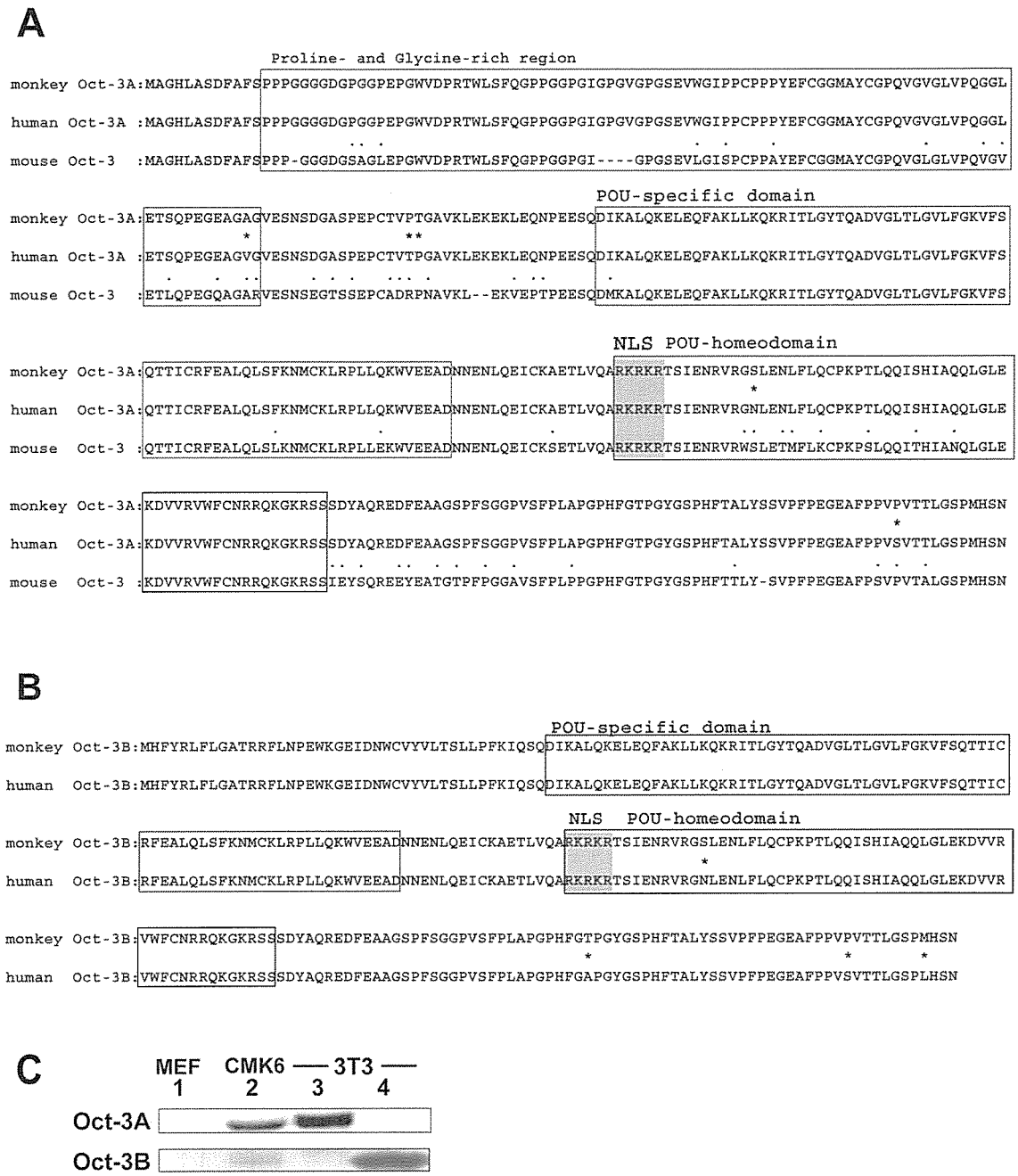


**FIG. 1.** Predicted amino acid sequences and protein expression of two cynomolgus monkey Oct-3 isoforms. Amino acid sequences of cynomolgus monkey Oct-3A (**A**) and Oct-3B (**B**) were predicted by their nucleic acid sequences. Both monkey Oct-3A and Oct-3B have high homologies to those of humans (98.6% and 98.5%, respectively). Asterisks (*) or dots (.) indicate amino acids that are different between human and monkey, or between human and mouse, respectively. Boxed sequences indicate the motifs in Oct-3, which are proline- and glycine-rich regions, POU-specific, and POU-homeo domains. These three motifs are common in monkey, human, and mouse. Monkey and human Oct-3A is the homolog of mouse Oct-3. Oct-3B does not have a proline- and glycine-rich region, although the POU-specific and POU-homeo domains, and nuclear localization signal (NLS) (gray) at the head of the POU-homeodomain, are common to Oct-3A and Oct-3B. The accession numbers for cynomolgus Oct-3A and Oct-3B in the DNA Data Bank of Japan (DDBJ) are AB243403 and AB243404, respectively. Protein expression of Oct-3 isoforms was examined by Western blotting (**C**). Cynomolgus ES cells (lane 2) expressed Oct-3B (*lower*) as well as Oct-3A (*upper*). Lanes 3 and 4 were Oct-3A and Oct-3B-transfected 3T3 cells used as positive controls: MEF (line 1) was used as a negative control. Oct-3A and Oct-3B were detected using the same anti-Oct-3 antibody whose epitope is common to both isoforms, on the same membrane with different exposure times.

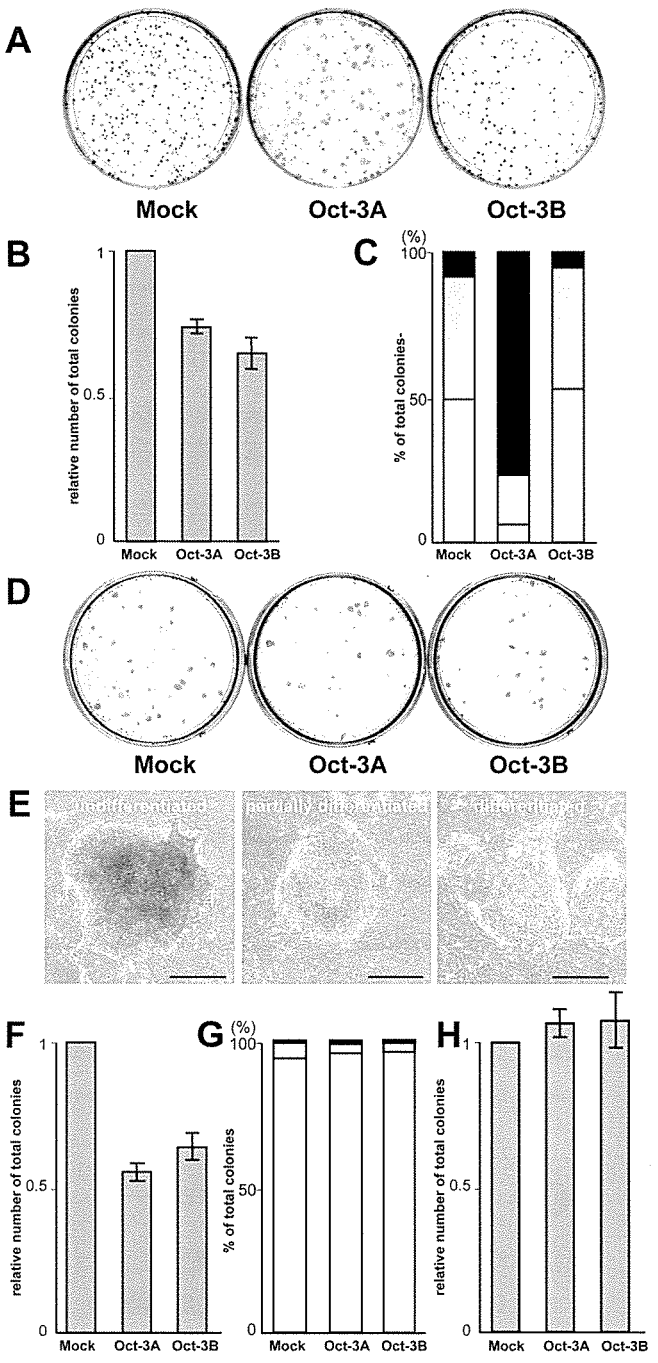


**FIG. 2.** Colony formation of ES cells followed by transfection of Oct-3A and Oct-3B expression vectors in mouse ES cells and cynomolgus ES cells. (**A**) The surviving colonies of mouse ES cells were detected and their undifferentiated state was examined by ALP staining. (**B**) The number of total colonies of Oct-3A- and Oct-3B-transfected mouse ES cells was scored as the relative number to that of empty vector (Mock)-transfected cells in each independently repeated experiment. The average scores are presented. (**C**) The average percentages of undifferentiated (white), partially differentiated (gray), and differentiated (black) colonies in each transfected group are shown. (**D**) ALP staining of colonies after G418 selection in cynomolgus monkey ES cells is presented. (Scale bar = 500 $\mu$m.) (**E**) Typical appearances of undifferentiated, partially differentiated, and differentiated colonies in monkey ES cells are shown. (**F**) The total colony number relative to Mock-transfected cynomolgus ES cells was scored and presented. (**G**) Undifferentiated (white), partially differentiated (gray), and differentiated (black) cynomolgus ES cell colonies were counted. The average percentages are shown. (**H**) The relative number of total colonies of cynomolgus ES cells transfected with the vectors that were cut between promoter and either Oct-3A or Oct-3B and that did not express exogenous Oct-3A or Oct-3B is shown.

were no differences in the number of colonies among these three groups following transfection of these vectors into cynomolgus ES cells (Fig. 2H). This implied that the reduced number of surviving colonies was due to the effects of exogenous Oct-3A and Oct-3B expression, but not due to differences in the plasmid transfection efficiency. These data suggest that the Oct-3A and Oct-3B up-regulation in monkey ES cells decreased survival or proliferation.

We assumed that the reduced total number of Oct-3A- and Oct-3B-transfected monkey ES colonies was caused by their differentiation, and that ES cells with high exogenous Oct-3 expression differentiate but do not proliferate. To examine this possibility, we quantified the Oct-3A and Oct-3B protein expression levels in stably transfected cynomolgus ES cell lines.

The protein expression level of Oct-3A stable transfectants was not more than 1.5 times that of nontransfected ES cells (wild-type) or mock-transfected cells. We screened the Oct-3A protein expression levels of 18 sta-

ble Oct-3A-transfected ES cell lines, but did not find any lines with higher Oct-3A expression. There was no apparent difference in Oct-3A protein levels between Oct-3A and mock-transfected clones (Fig. 3A). These data indicate that only the transfectants with an Oct-3A protein expression level similar to that of wild-type could survive and proliferate. This suggests that the appropriate level of Oct-3A for maintaining self-renewal and proliferation of monkey ES cells is restricted to a certain range, as in the case of Oct-3 in mouse ES cells (19), and that the high-level Oct-3A transfectants in monkey ES cells were probably eliminated during G418 selection.

In contrast, among Oct-3B stably transfected ES cell lines, several lines expressed high levels of Oct-3B (Fig. 3B). Of 11 stable Oct-3B transfected ES cell lines, seven clones had more than twice the Oct-3B expression level than the wild type, the highest being 4.9 times the wild-type level. On the other hand, the endogenous Oct-3A expression level was between 0.8 and 1.5 times that of the wild type. No correlation was detected between the expression level of Oct-3B and Oct-3A in any Oct-3B-transfected ES cell line.

### *Transient expression of Oct-3A promotes differentiation of monkey ES cells*

To elucidate whether Oct-3A or Oct-3B overexpression induces differentiation of monkey ES cells, we determined the expression of differentiation marker genes

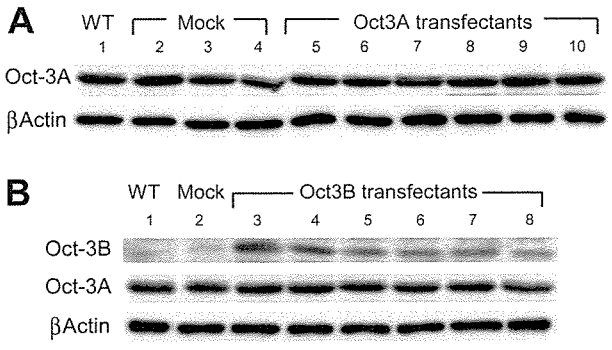


**FIG. 3.** Protein expression levels of Oct-3A or Oct-3B in cynomolgus ES cell lines transfected with Oct-3A and Oct-3B. (**A**) Oct-3A protein expression level of six different stable Oct-3A-transfected lines (lanes 5–10). Stable Oct-3A transfectants did not have apparently higher levels of Oct-3A expression than wild-type (WT) ES cells (lane 1) or Mock-transfected (lanes 2–4). (**B**) Oct-3B or Oct-3A protein expression level of six different stable Oct-3B-transfected lines (lanes 3–8). The stable Oct-3B transfectants had up to five-fold higher Oct-3B expression than WT (lane 1) and Mock-transfected cells (lane 2), whereas the Oct-3A expression levels were not different from WT or Mock-transfected cells. β-Actin was used as an internal control.

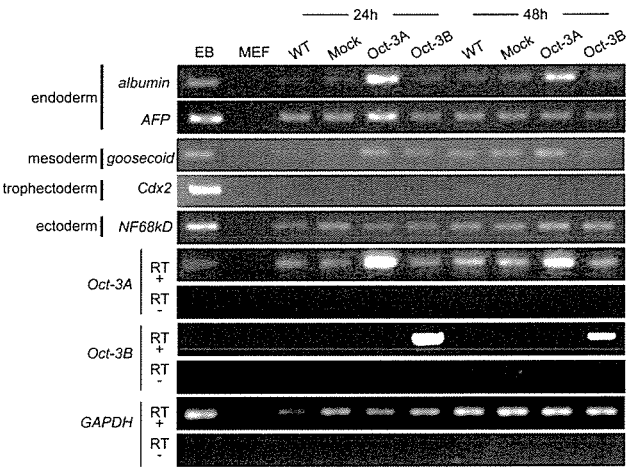


**FIG. 4.** Expression of differentiation marker in cynomolgus ES cells transiently transfected with Oct-3A and Oct-3B. Expression of the differentiation markers at 24 and 48 h after transfection of Oct-3A or Oct-3B was examined by RT-PCR. EB was used as a positive control for detecting differentiation markers. MEF was used as a negative control. Neither primer pair crossreacted with mouse cDNA. GAPDH was used as an internal control. RT+ and RT− indicate the presence and absence of reverse transcriptase in the first-strand cDNA reaction, respectively.

in monkey ES cells that were transiently transfected with either Oct-3A or Oct-3B vectors by RT-PCR. In the case of transient transfection, *Oct-3A* and *Oct-3B* expression levels peaked 48 h after transfection, and then decreased 72 h after transfection (data not shown). In Oct-3A transfectants, the endoderm markers, *alpha-fetoprotein (AFP)* and *albumin*, and the mesodermal marker, *goosecoid*, had a higher intensity 24 h after transfection than wild-type, mock, or Oct-3B transfectants (Fig. 4). The higher expression level of *albumin* and *goosecoid* in Oct-3A transfectants remained at 48 h after transfection. On the other hand, signal intensities of a trophectoderm marker, *Cdx2*, and an ectoderm marker, *NF68kD*, were not different between wild-type and any of the transfected cells. Differentiation marker expression was not different in Oct-3B-transfected cells compared to those of wild-type and mock-transfected cells. These data suggested that overexpression of Oct-3A, but not Oct-3B, in monkey ES cells promotes differentiation toward endodermal and mesodermal lineages.

## DISCUSSION

Oct-3 is a key regulator of early embryonic development and is important for maintaining self-renewal in mouse ES cells (18,19). In humans, there are two Oct-3 isoforms, Oct-3A and Oct-3B (25). Oct-3A is a homolog of mouse Oct-3, and they share 87% amino acid identity

(25). Oct-3B is a splicing variant of Oct-3A (25). In mouse, there is no isoform such as Oct-3B (25). There are no previous reports on the expression of Oct-3 isoforms or their functions in primate ES cells. In our study, we confirmed mRNA and protein expression of Oct-3 isoforms, Oct-3A and Oct-3B, in cynomolgus monkey ES cells, and determined that their sequences had high homology to the human Oct-3 isoforms.

The present study examined the effects of Oct-3A and Oct-3B overexpression on primate ES cells. The total number of surviving stable Oct-3A-transfected colonies was reduced to approximately 55% that of mock-transfected cells, and most of the surviving colonies remained in an undifferentiated state. Among the stably transfected monkey ES cell lines, none of the cell lines expressed high levels of Oct-3A. In the transient transfection assay, overexpression of Oct-3A in monkey ES cells induced an increase in endoderm and mesoderm markers. These data suggest that high Oct-3A expression promoted ES cell differentiation, and, therefore, cells with high Oct-3A expression do not proliferate or survive. In mouse ES cells, most of the surviving colonies were differentiated. It is possible that both mouse and monkey ES cells were differentiated due to Oct-3A overexpression, although the ratio of differentiated colonies were different between them. This might have been due to differences in viability of differentiated cells of each species. Alternatively, the Oct-3A-transfected primate ES cells might stop proliferation immediately after differentiation, whereas the Oct-3A transfected mouse ES cells might continue proliferation even after differentiation for a certain period.

We confirmed that Oct-3B is expressed in monkey ES cells at low but detectable levels. As in the case of Oct-3A, the total number of stable Oct-3B transfectants was reduced, and the ratio of undifferentiated colonies was not different from those of mock-transfected cells. Transient transfection of Oct-3B and RT-PCR analysis in monkey ES cells, however, failed to demonstrate any increase in the differentiation markers. Unlike Oct-3A transfection, several cell lines of stable Oct-3B transfectants had higher Oct-3B expression than wild-type ES cells. Therefore, Oct-3B overexpression might have had some influence on the viability of monkey ES cells, although it does not appear to have induced the differentiation of monkey ES cells. Stable Oct-3B-transfected monkey ES cell lines had up to five-fold higher Oct-3B expression than wild type. The amount of Oct-3B protein, however, was much smaller than that of Oct-3A, even in cells with the highest level of Oct-3B expression. Thus, Oct-3B overexpression might have little impact on the proliferation of monkey ES cells.

In summary, this is the first report of two Oct-3 isoforms, Oct-3A and Oct-3B, expressed in monkey ES cells. The overexpression of Oct-3A, but not Oct-3B, promoted differentiation of monkey ES cells into endodermal and mesodermal lineages. It is likely that there is a mechanism similar to that reported in mouse ES cells (19) to regulate the level of Oct-3A for maintaining self-renewal of primate ES cells. For further studies on the proper range of Oct-3A expression and the function of Oct-3B in primate ES cells, regulatable gene expression systems enable the control of Oct-3A and Oct-3B levels, including endogenous expression. Possible approaches include the combination of gene targeting of wild-type *POU5F1* alleles and an inducible system to control exogenous expression of Oct-3A or Oct-3B in primate ES cells.

## ACKNOWLEDGMENTS

This work was supported in part by grants from the National Bio-Resource Project, Ministry of Education, Culture, Sports, Science, and Technology (MEXT), Japan, and the Japan Society for the Promotion of Science.

## REFERENCES

1. Evans MJ and MH Kaufman. (1981). Establishment in culture of pluripotential cells from mouse embryos. Nature 292:154–156.
2. Bradley A, M Evans, MH Kaufman and E Robertson. (1984). Formation of germ-line chimaeras from embryo-derived teratocarcinoma cell lines. Nature 309:255–256.
3. Thomson JA, J Kalishman, TG Golos, M Durning, CP Harris, RA Becker and JP Hearn. (1995). Isolation of a primate embryonic stem cell line. Proc Natl Acad Sci USA 92:7844–7848.
4. Thomson JA, J Kalishman, TG Golos, M Durning, CP Harris and JP Hearn. (1996). Pluripotent cell lines derived from common marmoset (*Callithrix jacchus*) blastocysts. Biol Reprod 55:254–259.
5. Suemori H, T Tada, R Torii, Y Hosoi, K Kobayashi, H Imahie, Y Kondo, A Iritani and N Nakatsuji. (2001). Establishment of embryonic stem cell lines from cynomolgus monkey blastocysts produced by IVF or ICSI. Dev Dyn 222:273–279.
6. Thomson JA, J Itskovitz-Eldor, SS Shapiro, MA Waknitz, JJ Swiergiel, VS Marshall and JM Jones. (1998). Embryonic stem cell lines derived from human blastocysts. Science 282:1145–1147.
7. Takagi Y, J Takahashi, H Saiki, A Morizane, T Hayashi, Y Kishi, H Fukuda, Y Okamoto, M Koyanagi, M Ideguchi, H Hayashi, T Imazato, H Kawasaki, H Suemori, S Omachi, H Iida, N Itoh, N Nakatsuji, Y Sasai and N Hashimoto. (2005). Dopaminergic neurons generated from monkey embryonic stem cells function in a Parkinson primate model. J Clin Invest 115:102–109.
8. Boeuf H, C Hauss, FD Graeve, N Baran and C Kedinger. (1997). Leukemia inhibitory factor-dependent transcriptional activation in embryonic stem cells. J Cell Biol 138:1207–1217.

9. Matsuda T, T Nakamura, K Nakao, T Arai, M Katsuki, T Heike and T Yokota. (1999). STAT3 activation is sufficient to maintain an undifferentiated state of mouse embryonic stem cells. EMBO J 18:4261–4269.
10. Sumi T, Y Fujimoto, N Nakatsuji and H Suemori. (2004). STAT3 is dispensable for maintenance of self-renewal in nonhuman primate embryonic stem cells. Stem Cells 22:861–872.
11. Beattie GM, AD Lopez, N Bucay, A Hinton, MT Firpo, CC King and A Hayek. (2005). Activin A maintains pluripotency of human embryonic stem cells in the absence of feeder layers. Stem Cells 23:489–495.
12. Xu RH, X Chen, DS Li, R Li, GC Addicks, C Glennon, TP Zwaka and JA Thomson. (2002). BMP4 initiates human embryonic stem cell differentiation to trophoblast. Nature Biotechnol 20:1261–1264.
13. Ying QL, J Nichols, I Chambers and A Smith. (2003). BMP induction of Id proteins suppresses differentiation and sustains embryonic stem cell self-renewal in collaboration with STAT3. Cell 115:281–292.
14. Qi X, TG Li, J Hao, J Hu, J Wang, H Simmons, S Miura, Y Mishina and GQ Zhao. (2004). BMP4 supports self-renewal of embryonic stem cells by inhibiting mitogen-activated protein kinase pathways. Proc Natl Acad Sci USA 101:6027–6032.
15. Okamoto K, H Okazawa, A Okuda, M Sakai, M Muramatsu and H Hamada. (1990). A novel octamer binding transcription factor is differentially expressed in mouse embryonic cells. Cell 60:461–472.
16. Scholer HR, S Ruppert, N Suzuki, K Chowdhury and P Gruss. (1990). New type of POU domain in germ line-specific protein Oct-4. Nature 344:435–439.
17. Rosner MH, MA Vigano, K Ozato, PM Timmons, F Poirier, PW Rigby and LM Staudt. (1990). A POU-domain transcription factor in early stem cells and germ cells of the mammalian embryo. Nature 345:686–692.
18. Nichols J, B Zevnik, K Anastassiadis, H Niwa, D Klewe-Nebenius, I Chambers, H Scholer and A Smith. (1998). Formation of pluripotent stem cells in the mammalian embryo depends on the POU transcription factor Oct4. Cell 95:379–391.
19. Niwa H, J Miyazaki and AG Smith. (2000). Quantitative expression of Oct-3/4 defines differentiation, dedifferentiation or self-renewal of ES cells. Nature Genet 24:372–376.
20. Scholer HR, AK Hatzopoulos, R Balling, N Suzuki and P Gruss. (1989). A family of octamer-specific proteins present during mouse embryogenesis: evidence for germline-specific expression of an Oct factor. EMBO J 8:2543–2550.
21. Lenardo MJ, L Staudt, P Robbins, A Kuang, RC Mulligan and D Baltimore. (1989). Repression of the IgH enhancer in teratocarcinoma cells associated with a novel octamer factor. Science 243:544–546.
22. Scholer HR, GR Dressler, R Balling, H Rohdewohld and P Gruss. (1990). Oct-4: a germline-specific transcription factor mapping to the mouse t-complex. EMBO J 9:2185–2195.
23. Palmieri SL, W Peter, H Hess and HR Scholer. (1994). Oct-4 transcription factor is differentially expressed in the mouse embryo during establishment of the first two extraembryonic cell lineages involved in implantation. Dev Biol 166:259–267.
24. Yeom YI, G Fuhrmann, CE Ovitt, A Brehm, K Ohbo, M Gross, K Hubner and HR Scholer. (1996). Germline regulatory element of Oct-4 specific for the totipotent cycle of embryonal cells. Development 122:881–894.
25. Takeda J, S Seino and GI Bell. (1992). Human Oct3 gene family: cDNA sequences, alternative splicing, gene organization, chromosomal location, and expression at low levels in adult tissues. Nucleic Acids Res 20:4613–4620.
26. Niwa H, S Masui, I Chambers, AG Smith and J Miyazaki. (2002). Phenotypic complementation establishes requirements for specific POU domain and generic transactivation function of Oct-3/4 in embryonic stem cells. Mol Cell Biol 22:1526–1536.
27. Smith AE and KG Ford. (2005). Use of altered-specificity binding Oct-4 suggests an absence of pluripotent cell-specific cofactor usage. Nucleic Acids Res 33:6011–6023.
28. Cauffman G, H Van de Velde, I Liebaers and A Van Steirteghem. (2005). Oct-4 mRNA and protein expression during human preimplantation development. Mol Hum Reprod 11:173–181.
29. Hay DC, L Sutherland, J Clark and T Burdon. (2004). Oct-4 knockdown induces similar patterns of endoderm and trophoblast differentiation markers in human and mouse embryonic stem cells. Stem Cells 22:225–235.
30. Matin MM, JR Walsh, PJ Gokhale, JS Draper, AR Bahrami, I Morton, HD Moore and PW Andrews. (2004). Specific knockdown of Oct4 and beta2–microglobulin expression by RNA interference in human embryonic stem cells and embryonic carcinoma cells. Stem Cells 22:659–668.
31. Nagy A, J Rossant, R Nagy, W Abramow-Newerly and JC Roder. (1993). Derivation of completely cell culture-derived mice from early-passage embryonic stem cells. Proc Natl Acad Sci USA 90:8424–8428.
32. Niwa H, K Yamamura and J Miyazaki. (1991). Efficient selection for high-expression transfectants with a novel eukaryotic vector. Gene 108:193–199.

Address reprint requests to:
*Dr. Hirofumi Suemori*
*Laboratory of Embryonic Stem Cell Research*
*Stem Cell Research Center*
*Institute for Frontier Medical Sciences*
*Kyoto University*
*53 Kawahara-cho, Shogoin, Sakyo-ku*
*Kyoto, 606-8507, Japan*

*E-mail:* hsuemori@frontier.kyoto-u.ac.jp

Received January 30, 2006; accepted March 16, 2006.

*Acta Oto-Laryngologica* 2007; Suppl 557: 3–7

informa
healthcare

# Non-organic hearing loss

HARUKAZU HIRAUMI[1], JUN TSUJI[2], SHIN-ICHI KANEMARU[1], KIYOHIRO FUJINO[1] & JUICHI ITO[1]

[1]*Department of Otolaryngology-Head & Neck Surgery, Graduate School of Medicine, Kyoto University and* [2]*Department of Otolaryngology-Bronchoesophagology, Kyoto Medical Center, Kyoto, Japan*

**Abstract**

*Conclusion.* Most non-organic hearing loss (NOHL) patients were young females. The discrepancy between the results of pure tone audiometry and objective auditory testing suggests NOHL. The diagnostic problem is that objective audiometry is not included in routine examinations and we have to suspect NOHL in order to perform further examination. The correct diagnosis can be difficult in patients who present with unilateral sudden hearing loss or who also have moderate to profound organic hearing loss. *Objective.* Symptoms and results of auditory tests for NOHL patients were reviewed. *Patients and methods.* This study comprised 31 patients with NOHL. Age, symptoms, and the results of subjective and objective audiometry were collected. *Results.* Twenty-four patients were female and 7 were male. The age at attendance ranged from 7 to 39 years old, with an average age of 16.6 years. Eight patients received steroids before the correct diagnosis was made. Six of them presented with unilateral sudden hearing loss, and the other two patients had accompanying bilateral organic hearing loss.

**Keywords:** *Non-organic hearing loss, diagnosis, sudden hearing loss*

## Introduction

Non-organic hearing loss (NOHL) is a condition in which there is a discrepancy between the actual hearing threshold and admitted threshold of the patients. Various terms are used to describe this condition, including functional hearing loss, pseudohypacusis, psychogenic hearing loss, and conversion deafness. Some authors use these terms to describe different conditions [1], but the differences are obscure. The term NOHL is the most neutral one, and we use it in this paper. NOHL is a well-known clinical entity, but is often forgotten in the daily clinical setting. In most cases, the diagnosis of NOHL is easy, but in some cases the correct diagnosis is difficult and inappropriate treatments including steroid administration can be administered. Such diagnostic difficulty has not been mentioned in previous reports. In this manuscript, we review the etiology and the symptoms of NOHL patients and clarify the problems in the diagnosis of NOHL.

## Patients and methods

Thirty-one NOHL patients attended the Kyoto University Hospital Department of Otolaryngology-Head and Neck Surgery between April 1, 2000 and March 31, 2005. All patients underwent pure tone audiometry with AA-98 or AA-72 (RION). The diagnosis of NOHL is made when at least one of the following two characteristics is observed: (1) discrepancy between subjective and objective hearing evaluation test, and/or (2) clinically unexplainable audiological symptoms including prominent fluctuations of the threshold in the pure tone audiometry and lower threshold in speech audiometry than the threshold in the pure tone audiometry. Objective hearing thresholds are obtained using distortion product otoacoustic emissions (DPOAEs; CUBe-DIS II, Mimosa Acoustics) and/or auditory evoked brainstem response (ABR; MEB-2200, Nihon Kohden). Speech audiometry was performed using the 67-S word lists for Japanese.

Correspondence: H. Hiraumi, Department of Otolaryngology-Head and Neck Surgery, Graduate School of Medicine, Kyoto University, 54 Shogoin-Kawaharacho, Sakyo-ku, Kyoto 606-8507, Japan. Tel: +81 75 751 3346. Fax: +81 75 751 7225. E-mail: hhiraumi@ent.kuhp.kyoto-u.ac.jp

ISSN 0365-5237 print/ISSN 1651-2551 online © 2007 Taylor & Francis
DOI: 10.1080/03655230601065142

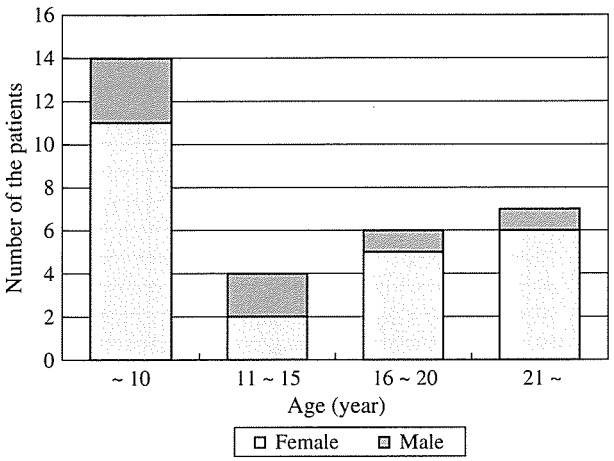


Figure 1. Number of patients according to their ages. Age at attendance ranged from 7 to 39 years old. Twenty-four patients were female and 7 were male. Most of the patients were young females.

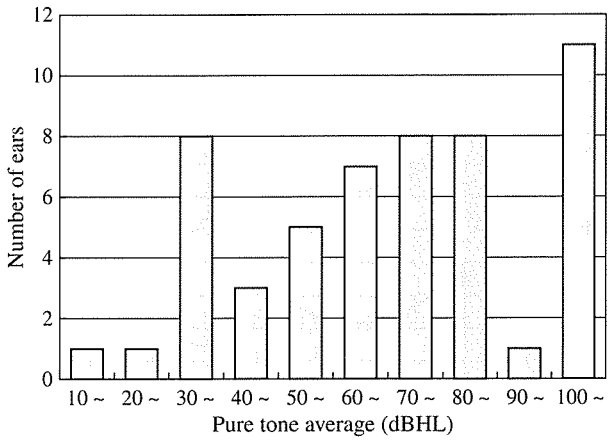


Figure 2. Number of ears according to their thresholds. The threshold distribution was trimodal, with a first peak at 30 dBHL, second peak at 70–80 dBHL, and third peak at >100 dBHL.

## Results

Twenty-four patients were female and 7 were male. The age at attendance ranged from 7 to 39 years old, with an average age of 16.6 years (Figure 1). Fifteen patients presented with sudden deterioration of hearing and/or tinnitus. Nine patients complained of progressive hearing loss. The other seven patients had no accompanying subjective symptoms and hearing loss was detected in the school screening hearing test or follow-up study for the organic hearing loss. Fourteen patients presented with unilateral hearing loss. Fourteen patients showed bilateral hearing loss. The other three patients had profound organic hearing loss in one ear and NOHL in the other ear. Among 14 unilateral NOHL patients, 8 patients developed contralateral NOHL afterwards. A total of 53 ears were diagnosed as NOHL.

The average pure tone audiometry threshold ranged from 16.7 dBHL to scale-out (Figure 2). The patterns of the pure tone audiograms were as follows: flat pattern in 33 ears, deaf pattern in 11 ears, hearing loss in both low and high frequencies in 5 ears, dip pattern in 2 ears, and hearing loss at high frequencies in 2 ears. Nine patients also had organic hearing loss: otitis media with effusion (three patients); large vestibular aquaduct syndrome (one); otosclerosis (one); endolymph hydrops (one); contralateral acoustic neurinoma (one); old idiopathic sudden sensorineural hearing loss (ISSNHL; one); and progressive sensorineural hearing loss (one). Seventeen patients were tested by DPOAEs, and 24 patients were tested by ABR. Thirteen patients underwent both DPOAEs and ABR testing. In total, 28 patients underwent an objective hearing test. In two patients DOPAEs failed to reveal NOHL because of inappropriate ear-piece insertion. In two patients, ABR was not able to reveal NOHL because of underlying organic hearing loss at high frequencies. Speech audiometry was performed in six patients. Four patients showed >90% speech discrimination at lower level than the threshold in the pure tone audiometry.

Twenty-four patients consulted other doctors first and were referred to our hospital, and 13 of them had received some kind of treatment. Seven patients were admitted to Kyoto University Hospital directly, and one of them was administered high-dose steroid therapy with the diagnosis of organic hearing loss. In total, 14 patients received inappropriate treatment before the diagnosis of NOHL, 8 of whom received steroids. In six of them, hearing loss emerged as unilateral sudden hearing loss, and the other two patients had accompanying bilateral organic hearing loss.

Three representative cases are described below.

### *Case 1*

A 33-year-old man presented with sudden progress of right tinnitus 4 days previously. The pure tone audiogram showed moderate to profound sensorineural hearing loss at all frequencies (Figure 3). He had contracted right ISSNHL 2 years earlier and received high-dose steroid therapy, leaving hearing loss between 250 Hz and 1000 Hz. Prior ISSNHL had been confirmed with DPOAEs, and recurrent hearing loss was suspected at first. However, the patient was very nervous about the deterioration of hearing, and he was tested with ABR. The ABR

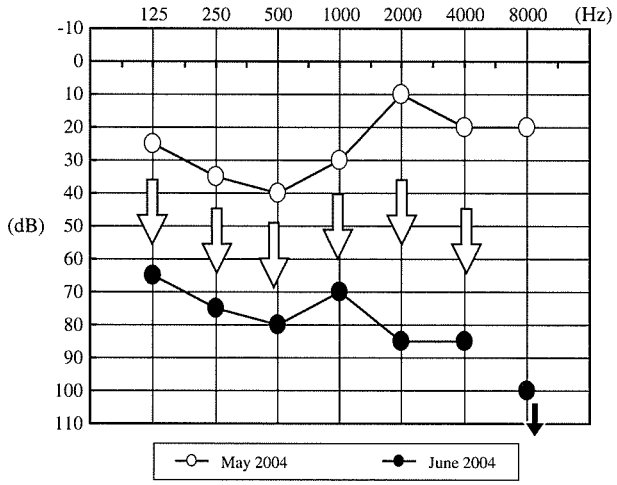


Figure 3. Pure tone audiogram of a 33-year-old patient who presented with sudden progress of right tinnitus (case 1). White circles indicate the threshold of the right ear on May 2002, and black circles on June 2004. The threshold elevated by 40–80 dB.

testing revealed significant wave V at 35 dBnHL, and he was diagnosed as having NOHL. Without any treatment, the pure tone threshold returned to the level before the progress of tinnitus.

*Case 2*

A 15-year-old boy presented with deterioration of right hearing level without subjective symptoms. He had been suffering from bilateral hearing loss because of bilateral large vestibular aqueduct. He had profound hearing loss in the left ear and moderate hearing loss in the right ear. He had been able to communicate with a hearing aid in the right ear, and the threshold had been stable. In routine hearing evaluation, the pure tone audiogram showed profound hearing loss in the right ear (Figure 4), and he was referred to our hospital. The ABR testing did not show wave V at 110 dBnHL. However, he did not complain about deterioration of hearing, and was able to communicate with the hearing aid as well as before. The pure tone threshold with hearing aid was evaluated, which showed that the elevation of threshold with hearing aid was minimum (Figure 5), and NOHL was highly suspected. The right ear is the only hearing ear, and we administered high-dose steroids. The pure tone threshold suddenly recovered to the prior level on the third day without subjective improvement of hearing.

*Case 3*

A 17-year-old girl presented to an otolaryngology department of another facility with sudden right

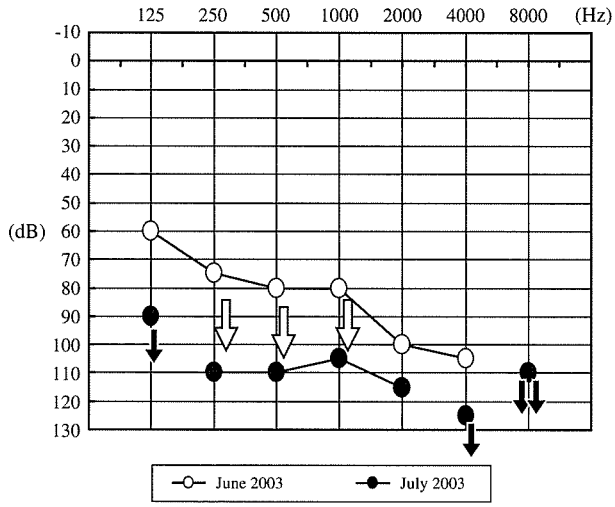


Figure 4. Pure tone audiogram of a 15-year-old patient without hearing aids (case 2). He had profound hearing loss in the left ear and moderate hearing loss in the right ear. In routine hearing evaluation, the pure tone audiogram showed profound hearing loss in the right ear. White circles indicate the threshold of the right ear on June 2003, and black circles indicate the threshold on July 2003. The threshold elevated by 15–35 dB.

hearing loss. The audiometric testing revealed profound sensorineural hearing loss on her right side. She was begun with high-dose steroids, and her hearing threshold returned to normal level. Since then, however, her hearing level in both ears deteriorated gradually. The hearing loss did not respond to steroids, and she was referred to Kyoto University Hospital. The pure tone audiogram showed bilateral profound sensorineural hearing loss with >90 dBHL threshold in both ears, and she complained that she was only able to

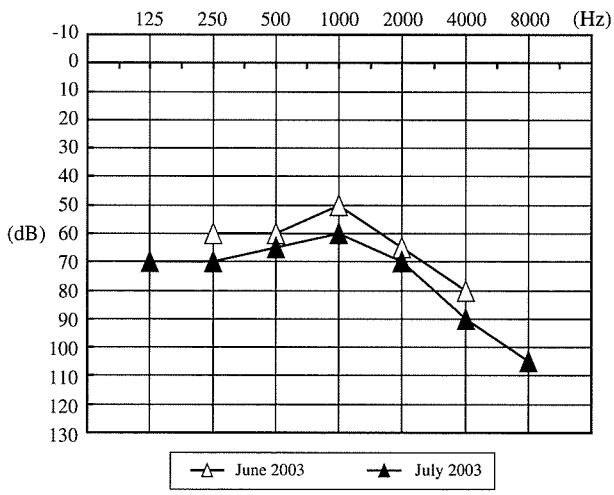


Figure 5. Pure tone audiogram of the same patient as in Figure 4 (case 2) with a hearing aid. The elevation of threshold with hearing aid was minimum and inconsistent with the pure tone audiogram without hearing aids (Figure 4).

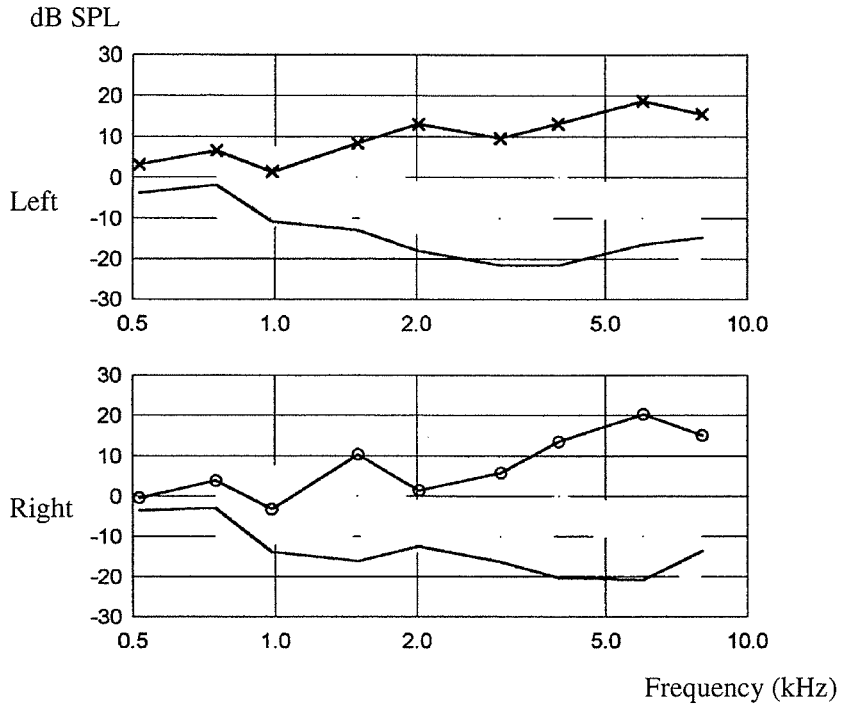


Figure 6. DPOAEs of a 17-year-old patient who presented with bilateral profound hearing loss showed good response in both ears (case 3). X symbols indicate the left ear responses and circles indicate right ear responses. The lines underneath the symbols show the noise level.

communicate through lip-reading. The DPOAEs showed normal response (Figure 6). In the ABR testing, the presence of wave V was observed at 15 dBnHL bilaterally (Figure 7). With the prescription of vitamin B12, she came to be able to communicate without lip-reading.

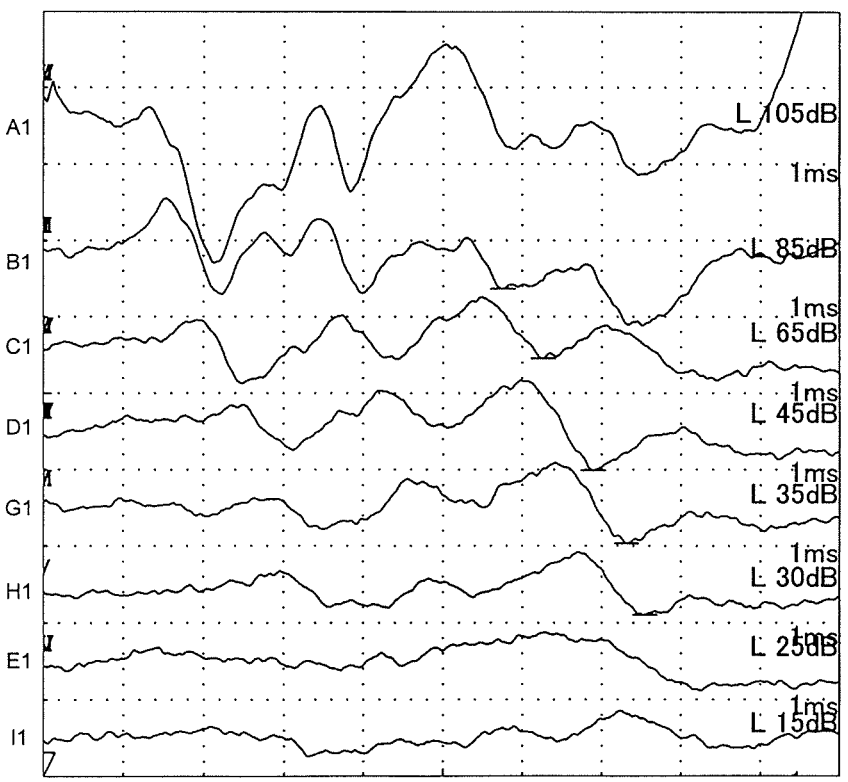


Figure 7. The ABR waveform of the same patient as in Figure 6 (case 3) showed a significant response at 15 dBnHL stimulation. This figure shows the result of the ABR with left ear stimulation. The ABR with right ear stimulation showed a similar response (not shown).

## Discussion

NOHL is a well-known clinical entity, but is often forgotten in the daily clinical setting and is sometimes misdiagnosed as organic hearing loss. The effectiveness of various objective hearing evaluations including ABR and DPOAEs has been reported in previous studies [2,3]. These objective hearing evaluation tests also revealed high sensitivity in our study (91.7% for ABR and 88.2% for DPOAEs). However, the problem is that these tests are not included in the routine auditory evaluation and we have to suspect NOHL in order to perform further examination. Qiu et al. [4] proposed a diagnostic plan for NOHL, but this plan did not provide a systematic strategy to suspect NOHL. In patients with bilateral moderate to profound NOHL, the discrepancy between the pure tone audiometry and patients' attitudes can be seen. They sometimes respond to small sound, and answer the questions with a small voice, which can be a cue to suspect NOHL. In other patients, a nervous attitude, diminished shadow hearing, or the unsteadiness of the pure tone threshold enable us to suspect NOHL. In the present study, most of the NOHL patients were young females and the pure tone audiogram showed flat or deaf pattern, consistent with previous studies [5,6]. This etiological result can be a help in suspecting NOHL, and the possibility of NOHL should be kept in mind in the diagnosis of young female patients with hearing loss showing flat or deaf pattern audiogram. However, in some cases, suspecting the NOHL is quite difficult. In our study, the diagnosis of NOHL was difficult in patients whose hearing loss emerged as unilateral sudden hearing loss and in those who had accompanying bilateral organic hearing loss.

In the diagnosis of unilateral NOHL, the differential diagnosis from ISSNHL is very important because high-dose steroids are often administered [7]. In our study, 12 patients presented with unilateral sudden onset hearing loss, and 6 of them were diagnosed as having ISSNHL and received steroids. In unilateral NOHL patients, the communication abilities and reaction to sounds cannot be a clue in the diagnosis [8]. In some patients, as we showed in case 3, the correct diagnosis was made after they developed bilateral NOHL. We have to keep in mind that NOHL presenting with unilateral sudden hearing loss is not uncommon.

The other problem in the diagnosis of NOHL is the concurrent organic hearing loss [9,10]. Some patients with progressive hearing loss show step-wise deterioration. In our case 1, the patient had experienced ISSNHL. We suspected the recurrence of hearing loss at first, but the patient showed a very nervous attitude and we suspected NOHL. The organic hearing loss was restricted at lower frequencies, which enabled us to reveal NOHL with ABR. Patients with moderate to profound hearing loss exhibit poor response in the objective hearing examination tests, and these tests may fail to reveal NOHL. In case 2, we were highly suspicious of NOHL. The sudden recovery without subjective improvement confirmed the diagnosis of NOHL. However, we were not able to prove NOHL with ABR before the treatment. In this case, the affected ear was the only hearing ear and we administered steroids, because we could not totally abandon the possibility of organic hearing loss. We think that administration of steroids is warranted in such cases.

## References

[1] Austen S, Lynch C. Non-organic hearing loss redefined: understanding, categorizing and managing non-organic behaviour. Int J Audiol 2004;43:449–57.

[2] Sanders JW, Lazenby BB. Auditory brain stem response measurement in the assessment of pseudohypoacusis. Am J Otol 1983;4:292–9.

[3] Durrant JD, Kesterson RK, Kamerer DB. Evaluation of the nonorganic hearing loss suspect. Am J Otol 1997;18:361–7.

[4] Qiu WW, Yin SS, Stucker FJ, Welsh LW. Current evaluation of pseudohypacusis: strategies and classification. Ann Otol Rhinol Laryngol 1998;107:638–47.

[5] Ishida T, Iwai K, Kuwashima S, Hirata S, Hosoya Y, Yokoyama T, et al. The clinical study of nonorganic hearing loss. Audiology Japan 1999;42:100–5.

[6] Tashiro T, Kanda Y, Kawajiri I, Tanigawa H, Kazama K, Kobayashi T. A clinical study on functional hearing loss in recent 10 years. Audiology Japan 1999;42:114–8.

[7] Salahaldin AH, Bener A, ElHakeem AA, Abdulhadi K. Management of idiopathic sudden sensorineural hearing loss: experience in newly developing Qatar. Int Tinnitus J 2004;10:165–9.

[8] Rotenberg BW, Makhija M, Papsin BC. Conversion disorder in a child presenting as sudden sensorineural hearing loss. Int J Pediatr Otorhinolaryngol 2005;69:1261–4.

[9] Radkowski D, Cleveland S, Friedman EM. Childhood pseudohypacusis in patients with high risk for actual hearing loss. Laryngoscope 1998;108:1534–8.

[10] Gelfand SA. Organic thresholds and functional components in experimentally simulated exaggerated hearing loss. Br J Audiol 1993;27:35–40.

*Acta Oto-Laryngologica* 2007; Suppl 557: 8–11

informa
healthcare

# c-Fos expression in the mouse brainstem after unilateral labyrinthectomy

JUN TSUJI, NORIHIKO MURAI, YASUSHI NAITO, & JUICHI ITO

*Department of Otolaryngology Head and Neck Surgery, Graduate School of Medicine, Kyoto University, Kyoto, Japan*

**Abstract**

*Conclusion.* The results indicated that the vestibular, prepositus hypoglossal, and inferior olive nuclei were activated after unilateral labyrinthectomy in mice like in other species. It is expected that the application of the present procedure to appropriate gene-deficient mice will elucidate the mechanism of the process of vestibular compensation. *Objective.* Vestibular compensation is attributed to functional and structural reorganization of neural networks in the central vestibular system, but its precise mechanism is still not clear. c-Fos protein is used as a marker of neuronal activation, because of its very limited expression in the normal state and rapid appearance after external stimulation. Previous reports, investigating c-Fos expression after unilateral labyrinthectomy were made in rats and guinea pigs, but not in the mouse brainstem. *Materials and methods.* For future application to the gene knockout mouse, we examined c-Fos expression in the mouse after unilateral labyrinthectomy. *Results.* Twenty-four hours after surgery, significantly increased c-Fos positive cells were observed in the bilateral medial vestibular nucleus (MVe), bilateral spinal vestibular nucleus (SpVe), contralateral prepositus hypoglossal nucleus (PrH), and contralateral inferior olive nucleus (IO).

**Keywords:** *Unilateral vestibular disturbance, vestibular compensation, c-Fos, mice*

## Introduction

Vestibular compensation after unilateral labyrinthectomy is an important phenomenon to understand plasticity of sensory and motor neurons in the central nervous system. Just after unilateral vestibular disturbance, spontaneous firing of type I neurons (which increases in firing rate for horizontal angular acceleration to the ipsilateral side) of the vestibular nuclear cells decreases in the disturbed side, which – combined with the increase in the affected side – leads to an extreme asymmetry. Such an event causes abnormal ocular motility even at rest, while in the compensation stage, spontaneous firing of type I neurons recovers to restore the difference described above [1,2]. Its precise mechanism is unclear. Suggested mechanisms include alteration of the innervation due to sprouting of synapses in the peripheral part [3], activation of commissural fibers between the bilateral vestibular nuclei in the central part, adaptation of the vestibular nuclei, and control from the cerebellum, although details are still not clear [1].

Immediate early gene *c-fos* and protein c-Fos is used as a marker of neuronal activation, because of its quite limited expression in the normal state and rapid appearance after some stimulation. Its expression is not completely coincident with the increase in electrophysiological neural activity, but is considered to reflect at least the increase in cellular activity [4]. Moreover, c-Fos protein is considered to induce expression of various genes [5]. Thus c-Fos induction may represent a biochemical process involved in the vestibular compensation.

Changes in the central nervous system in the stage of vestibular compensation have been studied using c-Fos protein in rats [4,6,7] and guinea pigs [8], and all of these studies reported c-Fos positive reactions in the medial vestibular nucleus (MVe), spinal vestibular nucleus (SpVe), and prepositus hypoglossal nucleus (PrH). It has also been reported that c-Fos positive cells are more prominent in the

Correspondence: Jun Tsuji, Department of Otolaryngology, Kyoto Medical Center, Fukakusamukaihatacho, Fushimi-ku, Kyoto 612-8555, Japan. Tel: +81 75 641 9161. Fax: +81 75 643 4325. E-mail: tsuji@ent.kuhp.kyoto-u.ac.jp

ISSN 0365-5237 print/ISSN 1651-2551 online © 2007 Taylor & Francis
DOI: 10.1080/03655230601065175

contralateral MVe and SpVe and in the ipsilateral PrH. Positive reactions have been also reported in the inferior olive nucleus (IO).

Recently, knockout animals deficient in receptors in the nervous system have been developed by gene manipulation, which are useful for investigation of actions of receptors. Among such animals, some are largely involved in vestibular compensation [9,10]. It is necessary to investigate vestibular compensation in mice in order to make use of such resources but less studies of vestibular compensation have been conducted in mice than in other species. In the present study, we determined expression of c-Fos after unilateral labyrinthectomy in mice for future application to the examination of vestibular compensation in knockout mice.

## Materials and methods

Eight C57BL/6 mice aged 6–10 weeks and weighing 15–30 g were used. The animals were anesthetized with xylazine HCl (9 mg/kg, i.p.) and ketamine (100 mg/kg, i.p.). Labyrinthectomy consisted of incision at the left postauricular part, identification of the ampullae of horizontal and posterior semicircular canals, drilling of each ampulla to make a small hole, confirmation of lymph leakage, several runs of injection of 99.5% ethanol from the drill-out site, and aspiration. Control animals only underwent incision at the postauricular region. Twenty-four hours later, the animals were deeply anesthetized with sodium pentobarbital (60 mg/kg, i.p.) and transcardially perfused with physiological saline follwed by 4% paraformaldehyde. The dissected brainstems were transferred to a 30% sucrose solution in phosphate buffer (pH 7.4, 4°C) until they sank and 20 μm slices were made. For every seventh section, rabbit polyclonal anti-human c-Fos antibody and biotin-treated goat anti-rabbit IgG were used as the primary and secondary antibodies, respectively, to perform the ABC method followed by DAB staining for observation. This process was conducted according to the method described by Cho [11], although the time of reaction with each of the primary and secondary antibodies was reduced to 30 min. The nerve nucleus was identified using the atlas developed by Paxinos and Franklin [12]. The mean number of positive cells per slice was determined and the Mann-Whitney U test was used for analysis.

## Results

Figures 1 and 2 show tissues of representative samples. The sample from an animal with labyrinthectomy (Figure 1a) revealed positive cells in MVe and PrH in the intact side and SpVe in the operated side, although the sample from a control animal (Figure 1b) did not show any positive cells. Another sample from an animal with labyrinthectomy (Figure 2a) revealed positive cells in the IO on the operated side, but the control sample (Figure 2b) did not show any positive cells.

The quantitative comparison between labyrinthectomy and control groups (Figure 3) demonstrated that there were significantly more c-Fos positive cells in the MVe on both sides of animals with labyrinthectomy than control animals: 21.83 and 27.0 cells/slice in the operated and intact sides, respectively, of animals with labyrinthectomy, and 2.25 and 1.80 cells/slice, respectively, in control animals. The same result was obtained in SpVe: 16.89 and 6.18 positive cells/slice in the operated and intact sides, respectively, of animals with

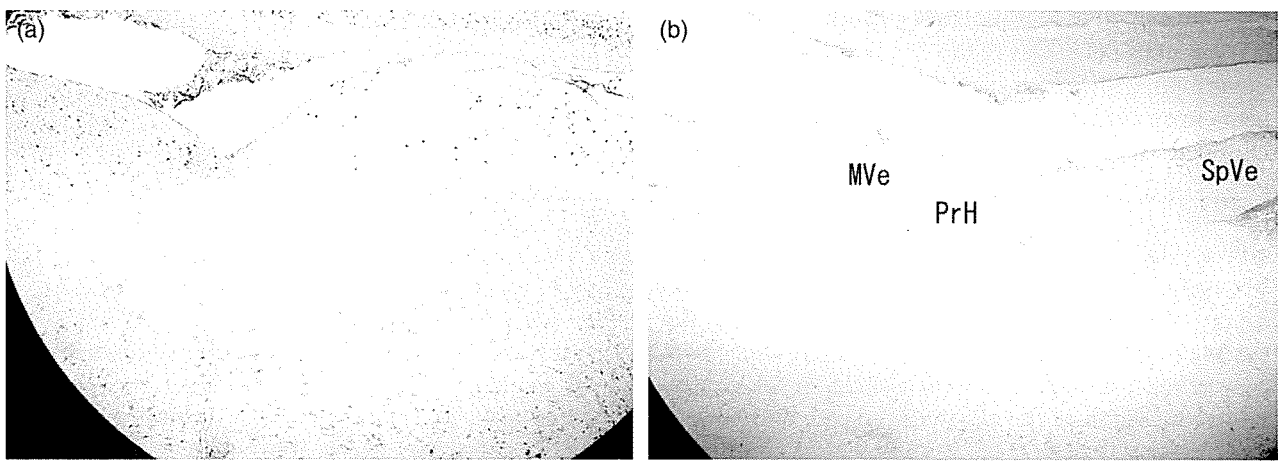


Figure 1. Expression of c-Fos positive cells in mice (C57BL/6) with labyrinthectomy. (a) Positive cells were observed in SpVe in the labyrinthectomy side, in bilateral MVe, and in PrH in the intact side. (b) Control. MVe, medial vestibular nucleus; PrH, prepositus hypoglossal nucleus; SpVe, spinal vestibular nucleus.